Evidence for the Need of Accurate Power Localization for Efficient Heating and Current Drive in TCV

T.P. Goodman for the TCV Team

Centre de Recherches en Physique des Plasmas
Association EURATOM-Confédération Suisse
Ecole Polytechnique Fédérale de Lausanne
CH-1015 Lausanne, Switzerland

email address of main author: timothy.goodman@epfl.ch

Abstract. The 6 beam 2nd harmonic X-mode (X2), 3MW, ECH/ECCD system of the TCV tokamak allows a fine tailoring of the deposition profiles in the plasma. The sensitivity of the sawtooth period to the deposition location is used to increase the equilibria reconstruction and ray-tracing accuracy. Off-axis ECH, followed by on-axis counter-ECCD produces improved central confinement regimes in which τ_{Ee} exceeds RLW scaling by a factor of 3.5. The PRETOR transport code (incorporating an RLW local transport model but constrained by the experimental density profiles) predicts an extreme sensitivity of τ_{Ee} to the deposition location of the counter-ECCD. This is confirmed by experiments. Sawtooth simulations using PRETOR, including the effects of current drive with inputs from the TORAY ray-tracing code, are in good agreement with experimental results. These results are an initial benchmark for the package of analysis codes, LIUQE / TORAY / PRETOR used during ECH/ECCD experiments on TCV.

1. Introduction

The Tokamak à Configuration Variable, TCV, (R_0 = 0.88m, a< 0.25m, B_T<1.45T, I_p < 1.2MA, κ_{vessel} = 3) is a medium-size device designed to study the influence of plasma shape on plasma stability and confinement. The only auxiliary heating capable of accessing all possible plasma shapes (e.g. $1.0 < \kappa_{achieved} < 2.8$ and $-0.7 < \delta_{achieved} < +0.7$) in the device is Electron Cyclotron Heating (ECH).

The auxiliary heating system of TCV is not limited to heating alone; but, is designed to provide an extremely flexible delivery system of antennas - or, “launchers” - capable of Electron Cyclotron Current Drive (ECCD), as well. The launchers have two degrees of freedom allowing the beams to be swept in a plane during a plasma shot: the plane of the sweep can be rotated between shots. In the usual setup, the plane of the sweep coincides with the poloidal plane of the tokamak and the rotation angle of the plane is used to introduce a toroidal injection angle for ECCD.

Although many present day plasma devices (both tokamaks and stellarators) are equipped with multi-source ECH systems, most often the power from several gyrotrons is combined in the launchers leaving a small number of independent beams in the plasma. In TCV the system consists of six 82.7GHz, 2.0s gyrotrons coupled to 6 independent launchers delivering a total of 2.7MW of power at the 2nd harmonic in X-mode (X2). In addition, three 118GHz, 210s gyrotrons are to be combined in one launcher at the top of the machine, providing 1.5MW of heating at the 3rd harmonic in X-mode (X3) in 2001. This frequency and launching configuration allows central heating at higher density than for X2 and has a high optical depth at the resonance. At present, a 118GHz gyrotron has been used with an X2 launcher for initial absorption tests [1].

With independent launchers, good alignment of the beams is crucial. Conversely, once precise aiming is confirmed, detailed comparisons between theory and experiment become possible. This paper is concerned with just such comparisons. In section 2, we discuss the alignment of the launchers and implications for the LIUQE [2] reconstruction code. A comparison of high temperature, improved central confinement (ICC) regimes [3,4] with the PRETOR [5] transport code is then given in section 3 and results of the successful simulation of experimental sawteeth by the sawtooth crash model [6] incorporated in the code, in section 4. Section 5 describes stable, sustained, fully non-inductive, ECCD plasma experiments, possible only with well aimed independent beams. Concluding remarks are made in section 6.

2. Reproducibility of the plasma/launcher geometry

To properly analyze the effects of ECH and ECCD on the TCV plasmas a good knowledge of the power deposition and current drive profiles is needed. This in turn requires an accurate overall reconstruction of the magnetic equilibrium and ray-tracing. These calculations are carried out using the LIUQE and TORAY [7] codes, respectively. Considerable work has been carried out to simplify the interface between the codes so that a typical 2s TCV shot can be analyzed and displayed graphically within 5-10 minutes.

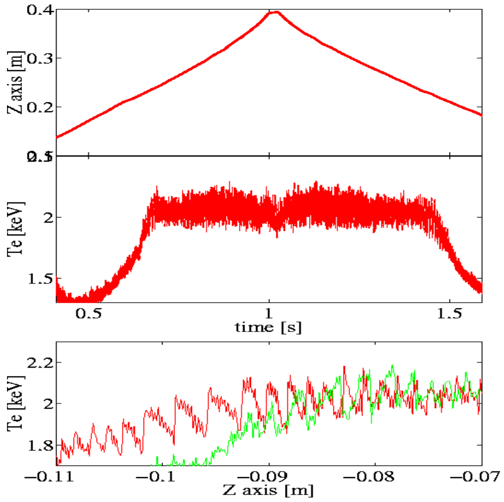

Fig. 1 The Plasma is swept through a stationary beam. The region of large sawteeth is displaced ~1.3cm when sweeping in opposite directions. The displacement is in the direction of the beam motion relative to the plasma center.

The accuracy of the overall reconstruction has been improved using measurements taken during sweeps of the plasma through the beam. In particular, the sawtooth period is highly sensitive to the power density close to the q=1, resulting in an effective spatial resolution smaller than the beam spot size and all of our present plasma diagnostics (mm vs. cm). This sawtooth response is very reproducible and the location of maximum sawtooth period is used as a target, to make a relative alignment between launchers to within ± 3mm [8,9]. This technique can thus provide an additional check on the magnetic reconstruction which helps improve the overall accuracy of ray-tracing results by showing the need for, and justifying the use of, tighter geometrical and numerical constraints in the code. Whereas ± 20mm accuracy in the Z_{axis} was previously acceptable in Ohmic discharges, this leads to excessively large errors in the deposition location calculated by ray-tracing.

Care must be taken to avoid confusion when moving the beams relative to the plasma (or vice verse) due to possible hysteresis effects. The hysteresis is often of the order of the error bars on the improved reconstruction and it is tempting to attribute the small differences in position of the large sawteeth to a residual error in the beam or plasma location. Figure 1 shows a situation in which the sweep direction appears to affect the location of the q=1 surface, near which the large sawteeth occur: A 1.3cm shift in the large sawtooth region is evident. This difference is small compared to the 3-4 cm resolution of diagnostics but would require only a 6mm error in the beam/plasma location to remove it altogether. Nevertheless, similar hysteresis has been confirmed with swept beams, plotting the sawtooth signal as a function of the launcher angle, i.e. independent of any reconstruction or ray-tracing. The hysteresis is also reproduced by PRETOR. These high resolution, reproducible results give us confidence that small, systematic changes in the launching angles can indeed be responsible for some of the significant changes in confinement observed during on-axis counter-ECCD - although the resolution of the ray-tracing is still limited. An example in which the limited resolution of the analysis codes prompted such systematic experiments, is that of the ICC regime.

3. The Improved Central Confinement Regime

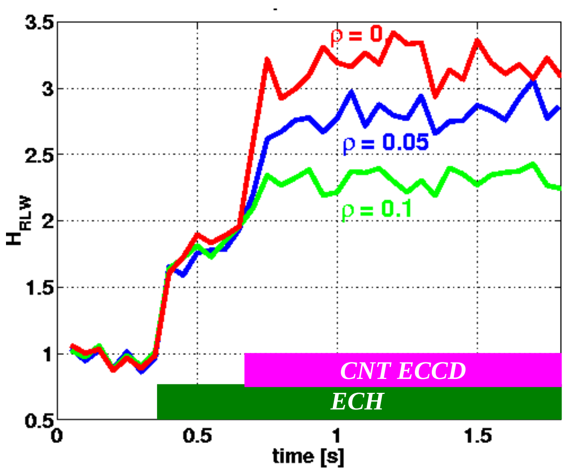

Fig. 2 Small changes in the deposition location, ρ, of central counter-ECCD in the ICC regime lead to large changes in global confinment,

The predictive, 1D, time dependent, transport code PRETOR, coupled with a 2D equilibrium solver and incorporating a Rebut-Lallia-Watkins (RLW) local transport model, has been validated on a wide variety of TCV L-mode plasmas [10]. When coupled to the TORAY code (for the power and driven current source terms), it successfully reproduces the evolution of the temperature profiles in many cases with auxiliary heating. Global RLW confinement scaling is appropriate for our low-n_e, high T_e/T_i plasmas [10], but is often exceeded for high-power central deposition[3,4]: A good figure-of-merit for these plasmas is the ratio $H_{RLW} = \tau_{exp.}/\tau_{RLW}$. The ICC regime is produced by a two step process: *1)* off-axis ECH is used to broaden the profiles and lower the central heat conductivity while maintaining the plasma stability when *2)* strong counter-ECCD is added, after ~300ms, on-axis[4]. PRETOR does not always successfully reproduce the experimental temperature evolution when taking the TORAY inputs as source terms. However, the code can be run in a “diagnostic mode”, in which *both* the n_e and T_e profiles are imposed and steady-state conditions (constant V_{loop}) are assumed. In this case, the deposition location is varied within the range permitted by the errors in the profile measurements, and a wide variety of current profiles and, therefore, safety factor profiles are obtained. These results highlight the extreme sensitivity of plasma performance to variations in the ECCD location, smaller than the accuracy or TORAY, and specifically suggests that exact on-axis counter-ECCD is crucial in producing the high temperatures and high confinements characteristic of this regime [11]. Figure 2 shows that this prediction is confirmed by experiments, in which changes of a few centimeters (as little as Δρ~0.05) cause ~15% changes in global confinement H_{RLW} factors.

4. Sawtooth simulations

PRETOR also includes a sawtooth crash model which has been used to successfully reproduce [11] the results of experiments in which the sawtooth period was found to depend on the local driven current as well as the power density near the q=1 surface [12]; an observation which, in turn, was used to put in evidence the asymmetric nature of off-axis current drive due to the poloidal field [8,9]. The sawtooth crash criterion included in the model can be written as $s_1 > s_{1\ crit}$, where s_1 is the shear in the profile of the safety factor at q=1 and $s_{1\ crit}$ is a critical value of shear above which the sawtooth instability is triggered. The density and temperature profiles are flattened out to the mixing radius after the crash. The q profile is relaxed according to the Kadomtsev model for full magnetic reconnection. The value of s_{1crit} contains a free parameter which is adjusted for a given experiment so that PRETOR reproduces the sawtooth period measured during the Ohmic phase: all free parameters are then fixed.

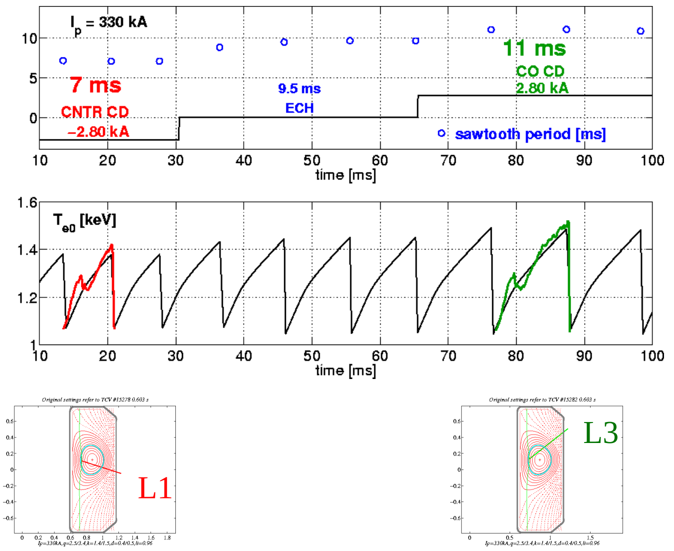

Fig. 3 Small changes in the local current drive (<1% of total current) cause measurable changes in the sawtooth period; an effect well reproduced by the sawtooth model used in PRETOR.

It is found that special care must be taken to reproduce the experimental situation when modeling sawteeth since all aspects found in experiments are important to the results: power density, sweep direction, current drive direction and magnitude. The model is however 1D and cannot reproduce features related to non-axisymemetric processes; e.g. magnetic islands. An example of a simplified case is shown in figure 3. In this situation, the beam location was fixed; however, different launchers were used in the two shots shown. The projection o the beam **k**-vector onto the poloidal field is different in the two cases, producing opposite driven currents; counter-ECCD in the case on the left and co-ECCD in the case on the right. A measured x-ray signal is superimposed on the simulated central temperature (scaled in the vertical, but not the horizontal, direction): the periods are in good agreement.

5. Fully non-inductive ECCD driven operation

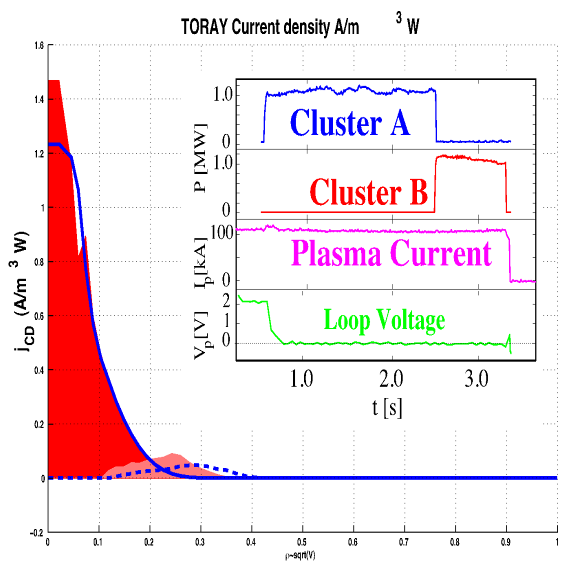

Fig. 4 Stable replacement one set of 2 beams, with another. This allows the pulse to be extended and demonstrates that exact beam overlap is not required. (blue - Launchers 1 & 3; red - Launchers 5 & 6).

The 6 independent beams allow a fine tailoring of the deposition profiles in the plasma and have allowed stationary fully ECCD driven plasmas to be produced in which the Ohmic transformer coil current I_{OH} is kept constant by the feedback system, rather than I_p, and the plasma has settled to the shape determined by the combination of the feed forward shaping-coil currents and the ECCD profiles - a process of current redistribution lasting several 100ms. In this mode of operation, the pulse length is determined by the gyrotron pulse length of 2s provided that the distribution of current sources is broad enough to prevent overpeaking of the profiles which otherwise lead to a disruption on an ideal-instability time scale. Up to 210kA have been driven in this way using all 6 gyrotrons [13].

As the total plasma current can be maintained non-inductively with as few as 2 beams, the sensitivity of the overall driven current to the profiles can be shown by switching from one current distribution to a slightly different one. This is done by replacing one pair of beams by two others with a 5ms overlap. The resulting 2.8s full ECCD plasma is shown in figure 4. This proof-of-principle experiment shows that it is possible to switch drivers during a pulse; something necessary in a reactor where one source may need to be taken off-line and be replaced by another. Since the plasma disrupts only after a few 10's of milliseconds if the gyrotrons are turned off, it should be possible to replace a source which has tripped off due to a malfunction, with another within this time. The fact that the sources are not exactly equivalent in location shows that small errors in alignment do not preclude a stable switch over. However, other, similar shots do disrupt. With the continual improvements being made in our analysis package, the differences between these shots should be able to be resolved.

6. Conclusions

Swept beam experiments have allowed (a) refinement in magnetic reconstruction analysis which in turn (b) reduces the errors in ray-tracing calculations and so (c) increases confidence that small differences in beam aiming can lead to large changes in plasma confinement as predicted by PRETOR. Careful experiments in the ICC regime confirm this with 15% decreases in confinement occuring for 5% displacements of deposition. Thus, the interplay of experiment and theory has resulted in methods of experimental design and analysis, using a package of codes and diagnostics, which increase our ability to properly study and predict the behaviour of ECH and ECCD dominated experiments, such as fully sustained ECCD plasmas.

Acknowledgment: This work was partly supported by the Swiss National Science Foundation.

References:

[1] ALBERTI, S., et al., post-deadline, this conference
[2] HOFMANN, F. and TONETTI, G., Nucl. Fusion **28** (1988) 1871.
[3] PIETRZYK, Z.A., et al., Phys. of Plasmas **7** (2000) 2909.
[4] PIETRZYK, Z.A., et al., subm. to Phys. Rev. Lett. and Lausanne Report LRP 678/00 (2000)
[5] BOUCHER, D. and REBUT, P.H., in *Proc. IAEA Tech. Conf. on Advances in Simulation and Modelling in Thermonuclear Plasmas*, 1992, Montréal (1993) 142.
[6] PORCELLI, F., et al., Plasma Phys. Contr. Fusion **38** (1996) 2163.
[7] SMITH, G.R., et al., in *Proceedings of the 9th Joint Workshop on ECE and ECRH, Borrego Springs, CA, 1995* (World Scientific, Singapore, 1995), p. 651.
[8] GOODMAN, T.P., et al., in *Proceedings of the 26th EPS Conf. on Contr. Fusion and Plasma Physics, Maastricht, 1999*, ECA (European Physical Society, Mulhouse, 1999), Vol. 23J, 1101.
[9] HENDERSON, M.A., et al., to be published in Fusion Engineering Design.
[10] POCHELON A. et al, Nucl. Fusion **39**, No 11Y (1999) 1807
[11] ANGIONI C. et al., to be published in *Theory of Fusion Plasmas, Varenna 2000* (Bologna: Editrice Compositori) and Lausanne Report LRP 682/00 (2000)
[12] GOODMAN T.P. et al., in *International Congress on Plasma Physics & 24th EPS(Proc. Cong. Prague, 1998)*, (European Physical Society, Geneva, 1998), Vol. 22c, 1324.
[13] CODA, S., et al., to be published in Plasma Phys. Contr. Fusion